Effects of nonuniform segment deformation on the constitutive relation of polymeric solids

Duan Z. Zhang,[1] Cheng Liu,[2] and Francis H. Harlow[1]
[1]*Theoretical Division, Fluid Dynamics Group T-3, B216, Los Alamos National Laboratory, Los Alamos, New Mexico 87545*
[2]*Materials Science and Technology Division, The Structure/Property Relations Group, MST-8, G755, Los Alamos National Laboratory, Los Alamos, New Mexico 87545*

(Received 11 March 2002; revised manuscript received 22 July 2002; published 22 November 2002)

A polymeric solid is modeled as a network of beads and strings. Beads in the polymer are divided into bead groups represented by the segment end points. Based on the equation of motion for each bead in the system, a macroscopic equation of motion for the polymer is derived. Velocity fluctuations of beads result in a pressure, the isotropic component of the stress, in the polymer. Interaction forces transmitted through segments connected to bead groups are the major source of the stress in the polymer. The tendency of segments to achieve their minima in Helmholtz free energy results in thermal elasticity of the polymer. Compared to the time scale of these segment interactions, other interactions among beads groups are short in time, therefore, result in a viscous stress. The motion of an average segment is modeled as an elastic spring immersed in a viscous fluid. The inertia of the segment is neglected because the viscous force is much larger than the inertial force. The governing equation for the deformation of the average segment is found to be a diffusion equation representing the balance between the viscous force and the elastic force in the segment. If the time scale of the macroscopic deformation is short compared to that of the deformation diffusion, the application of forces at both ends results in nonuniform deformation of the segment, which diffuses from the ends toward the center. This diffusion leads to relaxation of the macroscopic stress which we represent by a history integral. The kernel in the integral is asymptotic to $1/\sqrt{t}$ for a short time t, and is asymptotic to an exponentially decaying function for a long time t, in which t is the elapsed time from initiation of the deformation. This theoretically predicted kernel is observed in experiments conducted at constant temperature.

DOI: 10.1103/PhysRevE.66.051806 PACS number(s): 82.35.Lr, 83.10.Gr, 83.10.Bb

I. INTRODUCTION

A polymeric solid is regarded as a network of polymer chains consisting of chain segments and segment end points. Classical network theory neglects interactions of the chain segments with their surrounding medium, and the segment end points are regarded as permanent. To consider stress relaxation, classical network theory is typically extended in two ways. First is the transient network model. In such a model, junctions can be formed and broken [1], and the rate of the annihilation of the junction points is related to the stress relaxation in the material. The second approach is to consider the interactions of the polymer segments with their surrounding medium. The surrounding medium consists of side groups, dangling chains, small chain fragments, plasticizer molecules, and chains from other segments. These interactions were modeled as entanglement of chains in reptation models [2]. In a separate development, Schweizer [3,4] used a generalized Langevin-equation approach [5] to derive the equation of motion of a polymer chain. Advantages of Schweizer's approach includes the rigorous, at least conceptually, derivation of the equation of motion for polymer chains from fundamental principles such as the Liouville theorem in statistical mechanics. Based on the generalized Langevin equations, many transport coefficients, such as diffusivity and viscosity, were calculated through the study of the corresponding time-correlation functions (see, e.g., Ref. [6]). While these developments in the field of physical chemistry significantly advanced our understandings of the behavior of polymers, recent applications of polymeric material, especially for high-strain-rate applications, such as in Hopkinson bar experiments, require constitutive relations capable of capturing the dynamical behavior of the material. Knowledge of the transport coefficients, such as viscosities, elasticities, and diffusion coefficients, computed by integrating the time correlations throughout the entire history of motion, although important building blocks, is not sufficient for this purpose. This paper introduces a method to relate the macroscopic constitutive relations to the polymer chain motions at the molecular level. In this way, the method introduced in the present paper can take advantages of the physical understanding of polymers gained from the study of physical chemistry.

As a simple starting point, we simplify the generalized Langevin equation of motion for polymer chains [3]. We neglect inertial term in the equation and simplify the memory kernel as a δ function in time, because the time scale of interchain interactions in the polymer is short compared to the macroscopic time scale. As a result of this simplification, polymer gel can be modeled as a network of interconnected springs immersed in a viscous fluid. A similar physical model was used by Gurtovenko and Gotlib [7] to study polymeric solids. These authors divide the stress in the polymeric solid into three components, the elastic component resulting from the thermoelasticity of the chain segments, the viscous component resulting from the viscosity of the surrounding medium, and the component accounting for interactions between chains and the viscous medium. The network was assumed to be in a cubic form and the strain along a polymer segment was assumed to be uniform. The last assumption is actually present in all network theories about constitutive relations published in the literature except in a recent work

by Harstad *et al.* [8]. This assumption implies that the segment relaxation time τ is small compared to the time scale of the mean motion. In other words, the strain rate is small compared to $1/\tau$. As we shall see in this paper, the relaxation time τ can be about 450 to 1000 s for some polymers. Therefore the effects of nonuniform segment deformation can be significant for those polymers.

In the present paper, we examine the effects of nonuniform deformation of the polymer segments, as first described by Harstad *et al.* [8]. Our approach differs from theirs in that here we accomplish the multichain homogenization at the beginning of the derivation, whereas they developed a single chain description which then requires homogenization. In both approaches the effects of nonequilibrium arise from nonuniformity of chain deformations. Because the strain and therefore the force in the segment are not uniform, we must first determine the appropriate expression connecting the macroscopic stress and local forces in the polymer segments. Typically there are two approaches to derive the macroscopic stresses from the interaction forces at the molecular level. The first approach is to study the average force across an arbitrary plane in the polymer as described in the classical book by Bird *et al.* [9]. The second approach, which was first used by Irving and Kirkwood [10] in the derivation of the Navier-Stokes equation from the statistical mechanics, is directly related to the derivation of momentum equations of the system. This approach has been generalized to consider energy nonconserved systems such as particle interactions in granular and multiphase flows by Zhang and Rauenzahn [11,12], and Zhang and Prosperetti [13]. In the approach it is seen that the existence of stress relies on the action-and-reaction principle about the forces between an interacting pair of particles. When we consider forces acting on both ends of a polymer segment, the action-and-reaction principle does not apply directly, so that an additional generalization of the approach of Irving and Kirkwood is needed before the stress expression can be derived rigorously. This generalization is also useful for systems of distinguishable particles. This is explained in the following section and in Appendix A, in the process of derivation of our macroscopic equations.

In the derivation of macroscopic equations, we introduce a concept of bead groups, which contain one end point of polymer chains, together with the segments attached to that end point. Except for the loose end of a dangling chain, an end point is the position where chemical bonding joins chains strongly together. A single polymer chain may follow a tortuous pathway among its neighbor with multiple tie points that are permanent in the sense that one chain cannot be pulled through another. In contrast to the end point of the segment, these tie points can slide along a chain, contributing frictional and elastic forces. The contributions of these tie points to the effective elasticity and viscosity are not negligible. In our approach to the problem, we represent the polymer configuration by segments of each total chain and regard a tie point as if it were the end point of a segment. One aspect of the approximation introduced in this paper is that no distinction is made between the tie points and the end points. We acknowledge that tie points are more mobile than end points of a polymer chain. The approach we are taking in this paper also excludes topological effects related to changes in end points, such as may result from aging. The effects of changes in segment end points and tie points need to be considered as the theory undergoes further developments and refinements.

Under these approximations, macroscopic equations are derived by averaging over the equation of motion for the bead groups. Stress in the polymer system is expressed as contributions from three different physical origins. One of them comes from the random fluctuations of the beads in the polymer chains and is modeled as an isotropic pressure proportional to the absolute temperature of the polymer under the assumption that thermal relaxation of an individual bead is fast compared to the macroscopic strain. Interactions through segments connected to bead groups is another contributor to the stress. Because the segments are considered as permanent, the typical time scale of these interactions is long compared to that of other interactions among bead groups. The tendency of the segments to achieve their minima of Helmholtz free energies results in the thermal elasticity of the segments. Interactions between the beads in a segment and their surrounding beads are modeled as viscous frictions because of the time scale difference. An average segment is modeled as an elastic spring immersed in a viscous fluid. Different from the similar model used by Gurtovenko and Gotlib [7], we consider nonuniform deformation within the polymer segments. Other interactions among bead groups, such as friction among beads belonging to different bead groups, furnish another contribution to the macroscopic stress and result in a viscous component of the stress due to the transient nature of these interactions.

Because the motion of a polymer segment is dominated by the viscous force, the inertia of the elastic spring is neglected [3,4]. For a section of the average polymer segment, the difference in elastic forces at both ends is balanced by the viscous friction between the section and its surrounding medium. In this way the deformation of the spring satisfies a diffusion equation. This equation is solved in Sec. III. We then assume that the relaxation time of a segment is much longer than the time needed to propagate stress waves through the length of the polymer segment. Under this assumption an average polymer segment, the elastic spring, can be thought of being compressed (or pulled) at both ends at the same time. Strain of the average segment then diffuses toward the center of the segment. This diffusion of the strain leads to the history integral in the constitutive relation of the material. For a short time, the kernel in the history integral is proportional to the inverse square root of the time from the initiation of deformation $(1/\sqrt{t})$, while for a long time, the kernel approaches a decaying exponential. This implies significant stiffening for a high strain rate motion. For a low strain rate motion, the kernel can be approximated by a Maxwell model.

The relaxation time of an average segment is related to the length of the segment. The longer the segment is, the longer is the relaxation time. The effects of segment length distribution are studied in Sec. IV.

In Sec. V, we show experimental evidence of the theoreti-

cally predicted kernel, especially the $1/\sqrt{t}$ part for short times.

II. DYNAMICS OF THE NETWORK

We consider a solid polymer in which the polymer chains can be represented by strings and beads. Local strong interactions between polymer chains at isolated points are represented by junctions. A polymer segment is defined as a part of polymer chain that ends either at a junction point or at a free end. Let $\mathbf{y}^{(\alpha)}, \alpha = 1,2,\ldots,J$, be the positions of the segment end points and

$$\mathcal{J} = \{\mathbf{y}^1, \mathbf{y}^2, \ldots, \mathbf{y}^J\} \tag{2.1}$$

be the set of the positions of all segment end points, where J is the total number of segment end points in the system. This set contains not only junction points but also segment end points belonging to dangling chains and the end points of stray chains.

We denote $\mathbf{y}^{\gamma_{\alpha\beta}}$ to be the position of bead $\gamma_{\alpha\beta}$ between segment end points α and β. Let

$$\mathcal{S}_{\alpha\beta} = \{\mathbf{y}^1, \mathbf{y}^2, \ldots, \mathbf{y}^{N_{\alpha\beta}}\} \tag{2.2}$$

be the set of bead positions of the segment between ends α and β, in which $N_{\alpha\beta}$ is the number of beads in the segment excluding the end beads. Note that $\mathcal{S}_{\alpha\beta}$ is an empty set if α and β do not belong to the same segment or there is no bead in the string connected to both end points α and β. The topological structure of the polymer system is uniquely determined by the collection of sets consisting of set $\mathcal{J}$ and all sets $\mathcal{S}_{\alpha\beta}$.

Let $\mathcal{W}$ be the set of velocities $\mathbf{w}$ of beads in the system

$$\mathcal{W} = \{\mathbf{w}^1, \mathbf{w}^2, \ldots, \mathbf{w}^N\}, \tag{2.3}$$

where N is the total number of beads in the system. The dynamics of the system is uniquely determined by polymer configuration

$$\mathcal{C} = \mathcal{J} \times \prod \mathcal{S}_{\alpha\beta} \times \mathcal{W}, \tag{2.4}$$

and the equations of motion for beads in the polymer, where the product Π is over all sets $\mathcal{S}_{\alpha\beta}$.

Let $\mathbf{f}^{\alpha\beta}$ be the force acting on segment end point α from the segment connecting end points α and β, and $\mathbf{f}^{\alpha}$ be the other force acting on the segment end point α. The equation of motion for segment end point α can be written as

$$m_\alpha \frac{d\mathbf{w}^\alpha}{dt} = \sum_{\beta=1,\beta\neq\alpha}^{J} \mathbf{f}^{\alpha\beta} + \mathbf{f}^{\alpha}, \tag{2.5}$$

where m_α is the mass of bead α. The equation of motion for the beads between segment end points α and β can be written as

$$\sum_{\gamma_{\alpha\beta}=1}^{N_{\alpha\beta}} m_{\gamma_{\alpha\beta}} \frac{d\mathbf{w}^{\gamma_{\alpha\beta}}}{dt} = -\mathbf{f}^{\alpha\beta} - \mathbf{f}^{\beta\alpha} + \sum_{\gamma_{\alpha\beta}=1}^{N_{\alpha\beta}} \mathbf{f}^{\gamma_{\alpha\beta}}, \tag{2.6}$$

where $m_{\gamma_{\alpha\beta}}$ is the mass of bead $\gamma_{\alpha\beta}$ and $\mathbf{f}^{\gamma_{\alpha\beta}}$ is the force acting on bead $\gamma_{\alpha\beta}$, other than the force $\mathbf{f}^{\alpha\beta}$ and $\mathbf{f}^{\beta\alpha}$ from the segment end points α and β.

Let $\mathbf{F}_s^{\alpha\beta}$ and $\mathbf{F}_a^{\alpha\beta}$ be the symmetric and asymmetric parts of the interaction forces at both ends of the segment, defined as

$$\mathbf{F}_s^{\alpha\beta} = \frac{1}{2}(\mathbf{f}^{\alpha\beta} + \mathbf{f}^{\beta\alpha}), \quad \mathbf{F}_a^{\alpha\beta} = \frac{1}{2}(\mathbf{f}^{\alpha\beta} - \mathbf{f}^{\beta\alpha}). \tag{2.7}$$

With these definitions, we have

$$\mathbf{F}_s^{\alpha\beta} = \mathbf{F}_s^{\beta\alpha}, \ \mathbf{F}_a^{\alpha\beta} = -\mathbf{F}_a^{\beta\alpha}, \ \text{and} \ \mathbf{f}^{\alpha\beta} = \mathbf{F}_s^{\alpha\beta} + \mathbf{F}_a^{\alpha\beta}. \tag{2.8}$$

Using Eqs. (2.5)–(2.8), one finds

$$\frac{d}{dt}\left(m_\alpha \mathbf{w}^\alpha + \frac{1}{2} \sum_{\beta\neq\alpha} \sum_{\gamma_{\alpha\beta}=1}^{N_{\alpha\beta}} m_{\gamma_{\alpha\beta}} \mathbf{w}^{\gamma_{\alpha\beta}} \right) = \mathbf{F}^\alpha + \sum_{\beta=1,\beta\neq\alpha}^{J} \mathbf{F}_a^{\alpha\beta}, \tag{2.9}$$

where

$$\mathbf{F}^\alpha = \mathbf{f}^\alpha + \frac{1}{2} \sum_{\beta=1,\beta\neq\alpha}^{J} \sum_{\gamma_{\alpha\beta}=1}^{N_{\alpha\beta}} \mathbf{f}^{\gamma_{\alpha\beta}}. \tag{2.10}$$

The force $\mathbf{F}^\alpha$ defined in Eq. (2.10) and the momentum defined on the left side of (2.9) are summed over all beads in the segments that have an end point at α. The mathematical structure of these equations leads us to the definition of bead groups. For each point $\mathbf{y}^\alpha$ in set $\mathcal{J}$ of end points, we can define a group B_α of beads in the polymer system. A bead belongs to group B_α if the segment that the bead belongs to has an end point $\mathbf{y}^\alpha$. The mass of this bead group is

$$m_g^\alpha = m_\alpha + \frac{1}{2} \sum_{\beta=1,\beta\neq\alpha}^{J} \sum_{\gamma_{\alpha\beta}=1}^{N_{\alpha\beta}} m_{\gamma_{\alpha\beta}}. \tag{2.11}$$

These groups are not mutually exclusive. A bead in a segment belongs to two such groups since a segment always has two end points, and its mass is equally distributed to both groups it belongs. A bead at a segment end point belongs to only one group and its mass is owned entirely by that group as expressed in Eq. (2.11). In the following, we shall use this concept of bead groups to derived macroscopic equations and closure relations.

The average of a generic quantity $g^\alpha(\mathcal{C},t)$ associated with a segment end point is

$$n(\mathbf{x},t)\overline{g}(\mathbf{x},t) = \int \sum_{\alpha=1}^{J} \delta(\mathbf{x} - \mathbf{y}^\alpha) g^\alpha(\mathcal{C},t) P(\mathcal{C},t) d\mathcal{C}, \tag{2.12}$$

where $P(\mathcal{C},t)$ is the probability density function for polymer configuration $\mathcal{C}$ at time t and n is the number density of the segment end points defined by taking $g^\alpha = \overline{g} = 1$ in the Eq. (2.12). The probability $P(\mathcal{C},t)$ in Eq. (2.12) normalizes to 1; that is, its integral over all possible configurations is 1. The summation in Eq. (2.12) sums over all segment end points.

The pair distribution function $P_2(\mathbf{x}',\mathbf{x})$ for having a segment end point at position $\mathbf{x}$ and another end point at $\mathbf{x}'$ is

$$P_2(\mathbf{x}',\mathbf{x})=\sum_{\alpha=1}^{J}\sum_{\beta=1,\beta\neq\alpha}^{J}\int \delta(\mathbf{x}-\mathbf{y}^{\alpha})\,\delta(\mathbf{x}'-\mathbf{y}^{\beta})P(\mathcal{C},t)d\mathcal{C}. \tag{2.13}$$

The average $\langle g\rangle_2(\mathbf{x}',\mathbf{x})$, conditional on the requirement that each of the points $\mathbf{x}$ and $\mathbf{x}'$ is occupied by a segment end point, is

$$P_2(\mathbf{x}',\mathbf{x})\langle g\rangle_2(\mathbf{x}',\mathbf{x})=\sum_{\alpha=1}^{J}\sum_{\beta=1,\beta\neq\alpha}^{J}\int \delta(\mathbf{x}-\mathbf{y}^{\alpha}) \times\delta(\mathbf{x}'-\mathbf{y}^{\beta})g^{\alpha}(\mathcal{C},t)P(\mathcal{C},t)d\mathcal{C}. \tag{2.14}$$

By taking g^{α} as the momentum of bead group B_{α},

$$g^{\alpha}=m_{\alpha}\mathbf{w}^{\alpha}+\frac{1}{2}\sum_{\beta=1,\beta\neq\alpha}^{J}\sum_{\gamma_{\alpha\beta}=1}^{N_{\alpha\beta}} m_{\gamma_{\alpha\beta}}\mathbf{w}^{\gamma_{\alpha\beta}}, \tag{2.15}$$

we can express the mass flux as

$$\rho(\mathbf{x},t)\tilde{\mathbf{u}}(\mathbf{x},t)=n\overline{g}=\int\sum_{\alpha=1}^{J}\delta(\mathbf{x}-\mathbf{y}^{\alpha}) \times\left(m_{\alpha}\mathbf{w}^{\alpha}+\frac{1}{2}\sum_{\beta=1,\beta\neq\alpha}^{J}\sum_{\gamma_{\alpha\beta}=1}^{N_{\alpha\beta}} m_{\gamma_{\alpha\beta}}\mathbf{w}^{\gamma_{\alpha\beta}}\right) \times P(\mathcal{C},t)d\mathcal{C}, \tag{2.16}$$

where $\rho(\mathbf{x},t)$ is the mass density

$$\rho(\mathbf{x},t)=\int\sum_{\alpha=1}^{J}\delta(\mathbf{x}-\mathbf{y}^{\alpha})m_g^{\alpha}P(\mathcal{C},t)d\mathcal{C}. \tag{2.17}$$

Using a Liouville equation for the probability distribution function $P(\mathcal{C},t)$, one can derive a transport equation for quantity g^{α} as Eq. (8) in the paper by Zhang and Rauenzahn [11] or Eq. (2.40) in the paper by Zhang and Prosperetti [14]. By taking $g^{\alpha}=m_g^{\alpha}$, the transport equation becomes the continuity equation.

$$\frac{\partial\rho}{\partial t}+\nabla\cdot(\rho\overline{\mathbf{w}})=0, \tag{2.18}$$

where

$$\rho(\mathbf{x},t)\overline{\mathbf{w}}(\mathbf{x},t)=\int\sum_{\alpha=1}^{J}\delta(\mathbf{x}-\mathbf{y}^{\alpha})m_g^{\alpha}\mathbf{w}^{\alpha}P(\mathcal{C},t)d\mathcal{C}, \tag{2.19}$$

is the average momentum of segment end points, from which the average velocity $\overline{\mathbf{w}}(\mathbf{x},t)$ can be determined.

For g^{α} defined in Eq. (2.15), the transport equation becomes the averaged momentum equation for the material.

$$\frac{\partial\rho\tilde{\mathbf{u}}}{\partial t}+\nabla\cdot(\rho\tilde{\mathbf{u}}\cdot\overline{\mathbf{w}})=\nabla\cdot\boldsymbol{\sigma}^{R}+n\overline{\mathbf{F}^{\alpha}}+n\overline{\sum_{\beta=1,\beta\neq\alpha}^{J}\mathbf{F}_a^{\alpha\beta}}, \tag{2.20}$$

where

$$\boldsymbol{\sigma}^{R}=-\int\sum_{\alpha=1}^{J}\delta(\mathbf{x}-\mathbf{y}^{\alpha})\Bigg[m_{\alpha}(\mathbf{w}^{\alpha}-\overline{\mathbf{w}}) +\frac{1}{2}\sum_{\beta=1,\beta\neq\alpha}^{J}\sum_{\gamma_{\alpha\beta}=1}^{N_{\alpha\beta}} m_{\gamma_{\alpha\beta}}(\mathbf{w}^{\gamma_{\alpha\beta}}-\overline{\mathbf{w}})\Bigg] \times(\mathbf{w}^{\alpha}-\overline{\mathbf{w}})P(\mathcal{C},t)d\mathcal{C}, \tag{2.21}$$

is a stress due to velocity fluctuations of the beads in the system. In principle, the average velocities $\overline{\mathbf{w}}$ and $\tilde{\mathbf{u}}$ are not the same. Using Eq. (2.11) we can write the difference as

$$\rho(\tilde{\mathbf{u}}-\overline{\mathbf{w}})=\frac{1}{2}\int\sum_{\alpha=1}^{J}\delta(\mathbf{x}-\mathbf{y}^{\alpha})\sum_{\beta=1,\beta\neq\alpha}^{J}\sum_{\gamma_{\alpha\beta}=1}^{N_{\alpha\beta}} m_{\gamma_{\alpha\beta}} \times(\mathbf{w}^{\gamma_{\alpha\beta}}-\mathbf{w}^{\alpha})P(\mathcal{C},t)d\mathcal{C}. \tag{2.22}$$

By decomposing $m_{\gamma_{\alpha\beta}}(\mathbf{w}^{\gamma_{\alpha\beta}}-\mathbf{w}^{\alpha})$ into mean and fluctuating parts, expanding both the mean part of $m_{\gamma_{\alpha\beta}}(\mathbf{w}^{\gamma_{\alpha\beta}}-\mathbf{w}^{\alpha})$ and the probability $P(\mathcal{C},t)$ in Taylor series about $\mathbf{x}$, and then carrying out the integral, we can prove that Eq. (2.22) is of order ℓ^2/L^2, where ℓ is the typical segment length and L is an appropriate macroscopic length scale. The lower-order terms vanish because of the symmetry of the integration domain. If the macroscopic length scale is large compared to the molecular scale, this velocity difference (2.22) can be neglected. For this reason, we do not further distinguish velocities $\tilde{\mathbf{u}}$ and $\overline{\mathbf{w}}$ in the following text.

According to the definition (2.10) of $\mathbf{F}^{\alpha}$, the forces resulted from the interaction of the beads within the same group sum to zero because of the action and reaction principle. Therefore, $\mathbf{F}^{\alpha}$ is a result of interaction between different bead groups represented by their segment end points and can be written as

$$\mathbf{F}^{\alpha}=\sum_{\beta=1,\alpha\neq\beta}^{J}\mathbf{F}_g^{\alpha\beta}, \tag{2.23}$$

where $\mathbf{F}_g^{\alpha\beta}$ is the interaction force between bead groups B_{α} and B_{β}. If there is a segment connecting this pair of bead groups, the interaction force $\mathbf{f}^{\alpha\beta}$ transmitted through the segment is not included in $\mathbf{F}_g^{\alpha\beta}$. The group interaction force $\mathbf{F}_g^{\alpha\beta}$ satisfies Eq. (A12) in Appendix A. According to the extension of the theorem proven in Appendix A, we have

$$n\overline{\mathbf{F}^{\alpha}}=\nabla\cdot\boldsymbol{\sigma}^{V}, \tag{2.24}$$

$$\boldsymbol{\sigma}^{V}(\mathbf{x},t)=\frac{1}{2}\int\langle\mathbf{F}_g\rangle_2(\mathbf{x}',\mathbf{x},t)(\mathbf{x}'-\mathbf{x})P_2(\mathbf{x}',\mathbf{x},t)dx', \tag{2.25}$$

where $\langle \mathbf{F}_g \rangle_2$ is the average group interaction force between groups represented by segment end points at $\mathbf{x}'$ and $\mathbf{x}$. We note that the force $\langle \mathbf{F}_g \rangle_2$ represents the interactions among bead groups not transmitted through segments connecting them. These interactions are transient while the connection between bead groups are considered permanent. Therefore, the time scale of the variation of the force $\langle \mathbf{F}_g \rangle_2$ is short compared to that of force $\mathbf{f}^{\alpha\beta}$ transmitted through a segment connecting the pair of bead groups. This time scale difference enable us to model force $\langle \mathbf{F}_g \rangle_2$ as a viscous force as shown in the following section. We assume that the average force acting on a bead is proportional to the relative velocity between the bead and its surroundings. This assumption enables us to reprove Eq. (2.24) and to calculate the stress $\boldsymbol{\sigma}^V$ explicitly.

The force term defined in the last term of the right side of Eq. (2.20) can also be expressed as the divergence of a stress tensor after the use of the theorem extension proven in Appendix A.

$$\overline{n \sum_{\beta=1,\beta\neq\alpha}^{J} \mathbf{F}_a^{\alpha\beta}} = \nabla \cdot \boldsymbol{\sigma}^J, \tag{2.26}$$

$$\boldsymbol{\sigma}^J(\mathbf{x},t) = \frac{1}{2} \int \langle \mathbf{F}_a \rangle_2 (\mathbf{x}',\mathbf{x},t)(\mathbf{x}'-\mathbf{x}) P_2(\mathbf{x}',\mathbf{x},t) dx', \tag{2.27}$$

where $\langle \mathbf{F}_a \rangle_2(\mathbf{x}',\mathbf{x},t)$ is the asymmetric part of the average interaction force between the two end points $\mathbf{x}$ and $\mathbf{x}'$ of a segment. If the two end points do not belong to the same segment, the force is zero. Therefore, only those pairs connected by segments have contributions to the integral. To calculate this stress, we need to know the average forces at the ends of the segment. To calculate them, we can perform an ensemble average over all segments with end points at positions $\mathbf{x}$ and $\mathbf{x}'$. The average behavior of such segments can be modeled as an elastic spring immersed in a viscous fluid. The elasticity comes form the tendency of the average segment to achieve the minimum in Helmholtz free energy; and the viscosity comes from interactions of the beads in the segment with the surrounding beads not belonging to the same segment. In the following section, we calculate the average force between a segment and then use Eq. (2.27) to calculate this stress.

With Eqs. (2.26) and (2.24), and neglecting the difference between $\overline{\mathbf{w}}$ and $\tilde{\mathbf{u}}$, we can write the momentum equation (2.20) in the following conservation form:

$$\frac{\partial \rho \tilde{\mathbf{u}}}{\partial t} + \nabla \cdot (\rho \tilde{\mathbf{u}} \cdot \tilde{\mathbf{u}}) = \nabla \cdot (\boldsymbol{\sigma}^R + \boldsymbol{\sigma}^V + \boldsymbol{\sigma}^J). \tag{2.28}$$

With this momentum equation, we now see that the total stress in the polymer system contains three parts. The first part $\boldsymbol{\sigma}^R$ results from velocity fluctuations of the beads related to thermal motion. Both the second and the third parts represent interactions between bead groups. The second term $\boldsymbol{\sigma}^V$ represents the interaction between polymer segments belonging to different bead groups but not through segments connecting them. The third stress $\boldsymbol{\sigma}^J$ represents the interaction of bead groups through segments connecting them. The approach used in the derivation of the macroscopic equations (2.18) and (2.28) for the polymer system is an extension of a similar approach used by Zhang and Rauenzahn [11,12] and Zhang and Prosperetti [13] in the derivation of averaged equations for granular and two phase flows.

In the derivation of the momentum equation (2.28), there is an assumption that the typical polymer segment is much longer than a monomer and is much shorter than the macroscopic length scale. To proceed further beyond this point, both intersegment and intrasegment interaction models have to be introduced.

III. CLOSURE RELATIONS FOR THE STRESSES

A. Closure for $\boldsymbol{\sigma}^R$

According to definition (2.21), the stress $\boldsymbol{\sigma}^R$ is proportional to the correlation between the velocities of the beads in the segment and the velocities at the segment end points. For a long segment, only those beads close to an end point have velocities correlated to the velocity at the end point and have significant contributions to the stress. Therefore, only a small amount of mass in the polymer contribute to $\boldsymbol{\sigma}^R$ and this stress is small compared to the stress $\boldsymbol{\sigma}^J$, which is related to thermal motions of all beads in the segments.

Under the assumption of thermal equilibrium, the stress $\boldsymbol{\sigma}^R$ is proportional to the kinetic energy of the thermal motion and therefore proportional to the absolute temperature T of the system. If there is a perturbation about the thermal equilibrium, the velocity fluctuations of the beads cause momentum exchange across streamlines of the mean flow as in the kinetic theory of a gas [15]. This effect can be modeled as viscosity. While this effect is important in a dilute gas, this viscosity is small compared to the viscosity caused by friction among the polymer chains. Therefore, we can approximate the stress $\boldsymbol{\sigma}^R$ simply by a pressure proportional to the absolute temperature T and the density of the segment end points, which is proportional to the density defined in Eq. (2.17).

$$\boldsymbol{\sigma}^R = -C_R \rho T \mathbf{I}, \tag{3.1}$$

where C_R is a coefficient and $\mathbf{I}$ is the identity tensor. In a solid material, this stress is offset by elasticity of the material, since the strain of a material is defined to be zero at its equilibrium. Therefore, this pressure should be written as

$$\boldsymbol{\sigma}^R = \frac{\lambda_R}{1+\mathrm{tr}(\boldsymbol{\varepsilon})} \mathrm{tr}(\boldsymbol{\varepsilon}) \mathbf{I}, \tag{3.2}$$

where $\lambda_R = C_R \rho T$.

B. Closure for $\boldsymbol{\sigma}^V$

As mentioned in Sec. II, the stress $\boldsymbol{\sigma}^V$ represents interactions of beads in one group with beads in a different group. The dynamic nature of a polymer chain makes these interactions transient in time; and the time scale of this interaction is small compared to that of the interaction between bead

groups caused by a segment connecting them, because the segments are considered permanent between the two bead groups. The force acting on bead γ in a segment (including a segment end point) can be modeled as viscous friction and a random Brownian force $\mathbf{f}^b$ with zero mean [3,4,9,16],

$$\mathbf{f}^{\gamma} = -C_f m_{\gamma}[\mathbf{w}^{\gamma} - \mathbf{v}(\mathbf{y}^{\gamma})] + \mathbf{f}_b, \tag{3.3}$$

where C_f is a friction coefficient and $\mathbf{v}(\mathbf{y}^{\gamma})$ is the mean velocity of the surrounding medium experienced by bead γ. Thus $1/C_f$ has the dimension of time. This is the relaxation time of the bead γ in the surrounding viscous medium. This Langevin force is the starting point for a single-chain model, as derived by Harstad *et al.* [8]. For polymers such as polyisobutylene, at 217°C, if we take the bead size $a = 2.0$ Å, the bead mass of $m_{\gamma} = 56$ g/mol $= 9.3 \times 10^{-23}$ g, and the viscosity of the melt as $\mu = 10^5$ P as in the book by Rodriguez [17], the friction coefficient can be estimated using the Stokes drag law as $C_f = 6\pi\mu a/m = 4.1 \times 10^{20}$ s^{-1}. Although the Stokes drag law is only a rough approximation, the order of magnitude of C_f is expected to be meaningful.

We assume that a typical polymer segment length is short compared to the macroscopic length scale (i.e., $\ell/L \ll 1$). With this assumption the time difference for a perturbation to reach both ends of the segment is negligible compared to the macroscopic time scale. The velocity experienced by bead γ can be written as

$$\mathbf{v}(\mathbf{y}^{\gamma}) = \frac{1}{2}[\tilde{\mathbf{u}}(\mathbf{y}^{\beta}) + \tilde{\mathbf{u}}(\mathbf{y}^{\alpha})] + \mathbf{v}_r(\mathbf{y}^{\gamma}), \tag{3.4}$$

where $\mathbf{v}_r$ is an asymmetry function about the segment center representing the difference between the mean velocity experienced by a particle at $\mathbf{y}^{\gamma}$ and the average of the mean velocities experienced at both ends of the segment.

Using Eq. (3.3), and definitions (2.16) and (2.17), we can write the second term on the right side of Eq. (2.20) as

$$n\overline{\mathbf{F}^{\alpha}} = \frac{C_f}{4}\int \sum_{\alpha=1}^{J}\sum_{\beta=1}^{J} \delta(\mathbf{x} - \mathbf{y}^{\alpha}) m_{\alpha\beta} \times [\tilde{\mathbf{u}}(\mathbf{y}^{\beta}) - \tilde{\mathbf{u}}(\mathbf{y}^{\alpha})] P(\mathcal{J},t)\, d\mathcal{J}, \tag{3.5}$$

where $m_{\alpha\beta}$ denotes the total mass of segments with end points α and β and $P(\mathcal{J},t)$ is the probability distribution function of segment end points. This probability distribution function can be obtained by integrating over all degrees of freedom in $\mathcal{C}$ except those in $\mathcal{J}$. In the derivation of this equation, we have integrated over all degrees of freedoms other than the positions of the segment end points, and used the asymmetry property of $\mathbf{v}_r$.

Letting $G_{\alpha\beta} = m_{\alpha\beta}[\tilde{\mathbf{u}}(\mathbf{y}^{\beta}) - \tilde{\mathbf{u}}(\mathbf{y}^{\alpha})]$ in Eq. (A12), and using the theorem in Appendix A, we obtain Eq. (2.24) again; that is, the force $n\overline{\mathbf{F}^{\alpha}}$ can be expressed by the divergence of a stress. The stress is

$$\boldsymbol{\sigma}^V = \frac{C_f}{8}\int \sum_{\alpha=1}^{J}\sum_{\beta=1}^{J} \delta(\mathbf{x} - \mathbf{y}^{\alpha} + \mathbf{h}^{\alpha\beta}) m_{\alpha\beta} \times [\tilde{\mathbf{u}}(\mathbf{y}^{\beta}) - \tilde{\mathbf{u}}(\mathbf{y}^{\alpha})](\mathbf{y}^{\beta} - \mathbf{y}^{\alpha}) P(\mathcal{J},t)\, d\mathcal{J}, \tag{3.6}$$

where $|\mathbf{h}^{\alpha\beta}| < \ell$. In proving relation (2.24), we explicitly used the action-and-reaction principle. This principle is implicitly contained in Eq. (3.3) because the viscous force is expressed in terms of relative velocity. In Eq. (2.25), the force $\langle \mathbf{F}_g \rangle_2$ is the average interaction force between a pair of bead groups. Even if these two bead groups are not connected by a segment, the force is not necessarily zero. This force is modeled as friction acting on the beads as in Eq. (3.3). Therefore, in Eq. (3.6) the integral is over all segments. If the segment end points α and β are not connected by a common segment, $m_{\alpha\beta}$, and thus the integrand, vanishes.

Using Taylors expansion to calculate $\tilde{\mathbf{u}}(\mathbf{y}^{\beta}) - \tilde{\mathbf{u}}(\mathbf{y}^{\alpha})$ and keeping only the first term, we can write the stress $\boldsymbol{\sigma}^V$ as

$$\boldsymbol{\sigma}^V = \frac{C_f}{8}\nabla\tilde{\mathbf{u}}(\mathbf{x}) \int \sum_{\alpha=1}^{J}\sum_{\beta=1}^{J} \delta(\mathbf{x} - \mathbf{y}^{\alpha}) m_{\alpha\beta} \times (\mathbf{y}^{\beta} - \mathbf{y}^{\alpha})(\mathbf{y}^{\beta} - \mathbf{y}^{\alpha}) P(\mathcal{J},t)\, d\mathcal{J}. \tag{3.7}$$

At this point it is interesting to note that we only used the asymmetry of $\mathbf{v}_r$ in deriving $\boldsymbol{\sigma}^V$, and the actual distribution of $\mathbf{v}_r$ between the two segment end points has no effect on the stress $\boldsymbol{\sigma}^V$. In the following, we show that the distribution of $\mathbf{v}_r$ along the average segment affects the stress $\boldsymbol{\sigma}^J$.

We note that the integrand in Eq. (3.7) is a symmetric tensor, therefore, only the symmetric part of the velocity gradient has a contribution to $\boldsymbol{\sigma}^V$. With this, we have

$$\boldsymbol{\sigma}^V = \boldsymbol{\mu} \cdot \dot{\boldsymbol{\varepsilon}}, \tag{3.8}$$

where $\dot{\boldsymbol{\varepsilon}}$ is the rate of strain defined by

$$\dot{\boldsymbol{\varepsilon}} = \frac{1}{2}[\nabla\tilde{\mathbf{u}} + (\nabla\tilde{\mathbf{u}})^T], \tag{3.9}$$

and $\boldsymbol{\mu}$ is the symmetric viscosity tensor

$$\boldsymbol{\mu}(\mathbf{x},t) = \frac{C_f}{8}\int \sum_{\alpha=1}^{J}\sum_{\beta=1}^{J} \delta(\mathbf{x} - \mathbf{y}^{\alpha}) m_{\alpha\beta} \times (\mathbf{y}^{\beta} - \mathbf{y}^{\alpha})(\mathbf{y}^{\beta} - \mathbf{y}^{\alpha}) P(\mathcal{J},t)\, d\mathcal{J}. \tag{3.10}$$

This integral is over all segments with an end point at $\mathbf{x}$. Multiplying both sides of Eq. (3.10) by $1 = \int \delta(\mathbf{x} + \mathbf{r} - \mathbf{y}^{\beta}) d^3r$ and exchanging the order of integration, we have

$$\boldsymbol{\mu}(\mathbf{x},t) = \frac{C_f}{8}\int m_s(\mathbf{x},\mathbf{r},t)\mathbf{r}\mathbf{r}P_s(\mathbf{r},\mathbf{x},t)\, d^3r, \tag{3.11}$$

where m_s is the average segment mass between $\mathbf{x}$ and $\mathbf{x} + \mathbf{r}$, and $P_s(\mathbf{r},\mathbf{x},t)$ is the probability distribution function of finding a segment with end points at $\mathbf{x}$ and $\mathbf{x} + \mathbf{r}$,

$$P_s(\mathbf{r},\mathbf{x},t)=\int \sum_{\alpha=1}^{J}\sum_{\beta=1}^{J} \delta(\mathbf{x}-\mathbf{y}^{\alpha}) \times \delta(\mathbf{x}+\mathbf{r}-\mathbf{y}^{\beta})\chi_{\alpha\beta}P(\mathcal{J},t)d\mathcal{J}, \quad (3.12)$$

where $\chi_{\alpha\beta}=1$ if end points α and β are connected by a segment and $\chi_{\alpha\beta}=0$ otherwise.

If we assume that the polymer configuration around $\mathbf{x}$ is isotropic, that is, both m_s and P_s are spherically symmetric about $\mathbf{x}$, we can carry out the angular integral contained in Eq. (3.11) and the viscosity tensor can be represented by a scalar μ and Eq. (3.8) becomes

$$\boldsymbol{\sigma}^{V}=\mu\dot{\boldsymbol{\varepsilon}}, \quad \mu(\mathbf{x},t)=\frac{\pi}{6}C_f\int m_s(r,\mathbf{x},t)r^4P_s(r,\mathbf{x},t)dr. \quad (3.13)$$

C. Closure for $\boldsymbol{\sigma}^J$

Stress $\boldsymbol{\sigma}^J$ is the most important stress because it represents the force transmitted through polymer segments, the backbone of the polymer network. To calculate this stress using Eq. (2.27), we need to study the averaged equation of motion of a polymer segment. Under the assumptions that the interaction force between a polymer segment and its surrounding medium fluctuates very rapidly in time compared to the bulk motion of the polymer and that such interactions are statistically isotropic, the equation of motion for a bead in a polymer segment can be written as [3],

$$m_{\gamma_{\alpha\beta}}\frac{d\mathbf{w}^{\gamma_{\alpha\beta}}}{dt^2}=-\boldsymbol{\nabla}W(\mathbf{r}^{\gamma_{\alpha\beta}})-\boldsymbol{\eta}^{\gamma_{\alpha\beta}}(\mathbf{w}^{\gamma_{\alpha\beta}}-\mathbf{v})+\mathbf{F}^{\gamma_{\alpha\beta}}, \quad (3.14)$$

where W is the intrasegment potential of the mean force, $\boldsymbol{\eta}^{\gamma_{\alpha\beta}}$ is the friction constant, and $\mathbf{F}^{\gamma_{\alpha\beta}}$ is a random force.

Upon the ensemble average over all possible polymer segments connecting the end points α and β, we find the averaged equation of motion for the segments.

$$\frac{d\rho_s\mathbf{u}}{dt}=\frac{\partial\mathbf{N}}{\partial x}-C_f\rho_s(\mathbf{u}-\mathbf{v}), \quad (3.15)$$

where $\mathbf{N}$ is the average internal force in the segment, and the x axis is along the line connecting $\mathbf{y}^{\alpha}$ and $\mathbf{y}^{\beta}$.

In this equation, the time scale on the left side is the macroscopic time scale, while the relaxation time scale is $1/C_f$, which is much smaller than the macroscopic time scale, as mentioned in the preceding subsection. Therefore the effect of inertia, that is, the left side of Eq. (3.15), can be neglected.

The effect of the thermal motion represented by the Brownian force in Eq. (3.3), and the potential energy between neighboring beads, are represent by the Helmholtz free energy. The average force $N(\mathbf{x},t)$ at a point in the segment can be calculated from the free energy [9] as

$$\mathbf{N}=k_0\frac{\partial\boldsymbol{\lambda}}{\partial x}, \quad (3.16)$$

where $\boldsymbol{\lambda}$ is the displacement relative to the center of the polymer segment and k_0 is the elasticity coefficient proportional to absolute temperature T.

$$k_0=C_kkT/\ell=C_kkT\rho_s/m_s, \quad (3.17)$$

where C_k is a coefficient, m_s is the mass of the segment, and $k=1.3807\times10^{-23}$ J/K is the Boltzmann constant.

Using Eq. (3.16) in the frame fixed at the segment center, the momentum equation can be written as

$$k_0\frac{\partial^2\boldsymbol{\lambda}}{\partial x^2}-C_f\rho_s(\mathbf{u}-\mathbf{v})=0. \quad (3.18)$$

The velocities in this equation are the velocities relative to the segment center. Symmetry about the average segment and about the center requires that both velocities $\mathbf{u}$ and $\mathbf{v}$ be asymmetrical about the mass center. We assume that the average segment has no shearing and bending strength and deformation of the segment is along the axis connecting $\mathbf{y}^{\alpha}$ and $\mathbf{y}^{\beta}$. These velocities represent the mean deformation rates of the average segment and its surroundings. We assume that these deformation velocities are linearly related, or

$$\mathbf{u}-\mathbf{v}=C\mathbf{u}, \quad 0\leqslant C\leqslant 1, \quad (3.19)$$

where C is a constant along the segment. In this way, we see that the last term of Eq. (3.18) represents the resistance to the segment deformation from its surroundings.

As a first approximation, we neglect nonlinear effects and write

$$\mathbf{u}=\frac{\partial\boldsymbol{\lambda}}{\partial t}. \quad (3.20)$$

With these approximations, the equation for the displacement field can be written as

$$\frac{\partial\boldsymbol{\lambda}}{\partial t}=\frac{\ell^2}{4\tau}\frac{\partial^2\boldsymbol{\lambda}}{\partial x^2}, \quad (3.21)$$

where ℓ is the length of the segment and

$$\tau=\frac{\ell^2\rho_sC_fC}{4k_0}=\frac{\ell^3m_sC_fC}{4C_kkT}. \quad (3.22)$$

For a segment consisting of 100 polyisobutylene monomers, the segment length can be estimated as 400 Å, and the relaxation time at temperature 217 °C can be estimated to be about 450 s if we assume the coefficient $C/C_k=0.5$. Although at this temperature polyisobutylene is in the melt form, the segment relaxation time is still meaningful. For polyisobutylene gel, the viscosity is expected to be much larger, and therefore the segment relaxation time is expected to be much longer. This rough estimation of segment relaxation time suggests that even for fairly small macroscopic strain rate, say 10^{-3} s^{-1}, the effects of nonuniform deformation could be significant.

The boundary and initial conditions for this equation can be written as

$$\mathbf{u}(\ell/2,t)=\mathbf{u}_e(t), \quad \boldsymbol{\lambda}(0,t)=\boldsymbol{\lambda}(x,0)=0, \tag{3.23}$$

where $\mathbf{u}_e(t)$ is the average velocity relative to the mass center of the segment. Under the assumption that the average position of the segment forms a straight line connecting both segment end points, and that the force **N** acts along the straight line, the force **N** acting on the end of the segment can be obtained by solving Eq. (3.21) with boundary and initial conditions (3.23). Detailed procedure of solving this equation is described in Appendix B. The magnitude of the force is calculated as

$$N(\ell/2,t)=\frac{2k_0}{\ell}\left[\int_0^t u_e(t')dt'+\int_0^t u_e(t')K_r\left(\frac{t-t'}{\tau}\right)dt'\right], \tag{3.24}$$

or equivalently (by changing integration variable $t''=t-t'$ and then denoting t'' as t')

$$N(\ell/2,t)=\frac{2k_0}{\ell}\left[\int_0^t u_e(t')dt'+\int_0^t u_e(t-t')K_r\left(\frac{t'}{\tau}\right)dt'\right], \tag{3.25}$$

where

$$K_r\left(\frac{t}{\tau}\right)=\sqrt{\frac{\tau}{\pi t}}\left[1+2\sum_{k=1}^{\infty}\exp(-k^2\tau/t)\right]-1. \tag{3.26}$$

As proven in Appendix B, the kernel K_r goes to zero as time goes to infinity. This kernel describes fading memory of the segments. With this result, the forces $\langle\mathbf{F}_s\rangle_2$ and $\langle\mathbf{F}_a\rangle_2$ averaged over all the segments with the same segment end points in the ensemble can be written as

$$\langle\mathbf{F}_s\rangle_2=\mathbf{0} \quad \text{and} \quad \langle\mathbf{F}_a\rangle_2=\mathbf{N}(\ell/2,t). \tag{3.27}$$

If points $\mathbf{x}$ and $\mathbf{x}+\mathbf{r}$ are not connected by a segment, the force between them is considered zero. With such conditional average the stress $\boldsymbol{\sigma}^J$ described in Eq. (2.27) can be written as

$$\boldsymbol{\sigma}^J(\mathbf{x},t)=\frac{1}{2}\int \mathbf{N}\left(\frac{\ell}{2},t\right)\mathbf{r}P_s(\mathbf{r},\mathbf{x},t)d^3r. \tag{3.28}$$

We now assume that the motion of the average segment is affine, so that the average velocity $\mathbf{u}_e$ is related to the macroscopic stain rate $\dot{\boldsymbol{\varepsilon}}$ as

$$u_e(t)=\frac{\ell}{2}(\dot{\boldsymbol{\varepsilon}}\cdot\mathbf{n})\cdot\mathbf{n}, \tag{3.29}$$

where $\mathbf{n}=\mathbf{r}/r$. We note that the relaxation time defined in Eq. (3.22) is a function of the segment length $\ell=r$. Substituting Eq. (3.29) into Eq. (3.25) and then into Eq. (3.28), leads to

$$\sigma_{ij}^J=\frac{1}{2}k_0\varepsilon_{pq}(t)\int n_pn_qn_in_jP_s(r,\mathbf{x},t)r^3drd\Omega + \frac{1}{2}k_0\int_0^t\dot{\varepsilon}_{pq}(t-t') \times\left[\int n_pn_qn_in_jK_r\left(\frac{t'}{\tau(r)}\right)r^3P_s(r\mathbf{n},\mathbf{x},t)drd\Omega\right]dt', \tag{3.30}$$

where Ω is the solid angle. If we assume that the pair distribution is spherically symmetric, we can carry out the angular integral to find

$$\boldsymbol{\sigma}^J=\lambda_0[\mathrm{tr}(\boldsymbol{\varepsilon})\mathbf{I}+2\boldsymbol{\varepsilon}]+\lambda_0 \times\int_0^t\{\mathrm{tr}[\dot{\boldsymbol{\varepsilon}}(t-t')]\mathbf{I}+2\dot{\boldsymbol{\varepsilon}}(t-t')\}\overline{K}_r(t')dt', \tag{3.31}$$

where

$$\lambda_0=\frac{2\pi}{15}k_0\int r^3P_s(r,\mathbf{x},t)dr \tag{3.32}$$

and

$$\overline{K}_r(\mathbf{x},t)=\frac{\int K_r\left(\frac{t}{\tau(r)}\right)r^3P_s(r,\mathbf{x},t)dr}{\int r^3P_s(r,\mathbf{x},t)dr}. \tag{3.33}$$

Using Eq. (B18) in Appendix B, we see that

$$\lim_{t\to\infty}\overline{K}_r(\mathbf{x},t)=0. \tag{3.34}$$

Relaxation of the kernel $\overline{K}_r$ represents the fading memory of the polymer material. Equation (3.33) implies that the macroscopic relaxation is determined by the distribution of polymer segment length. To understand the properties of the kernel $\overline{K}_r$, we first study the properties of the kernel K_r for a fixed segment length with a fixed relaxation time. Using Eq. (B17), we can show that, as t approaches zero, K_r approaches $\sqrt{\tau/\pi t}$. The function K_r is plotted in Fig. 1. As shown in Fig. 1, a good approximation of K_r can be written as

$$K_r\left(\frac{t}{\tau}\right)=\begin{cases}\sqrt{\tau/(\pi t)}-\mathrm{erf}(\sqrt{\tau/t}) & \text{if } t<0.15\tau\\ Ae^{-t/\tau_a} & \text{otherwise,}\end{cases} \tag{3.35}$$

where $A\approx 2.00$ and $\tau_a\approx 0.101\tau$. This implies that, at the exponential decay region of K_r, the relaxation time of the exponential decay is about an order of magnitude smaller than τ.

For $\overline{K}_r$, using Eq. (B17), we can show for any segment length distribution,

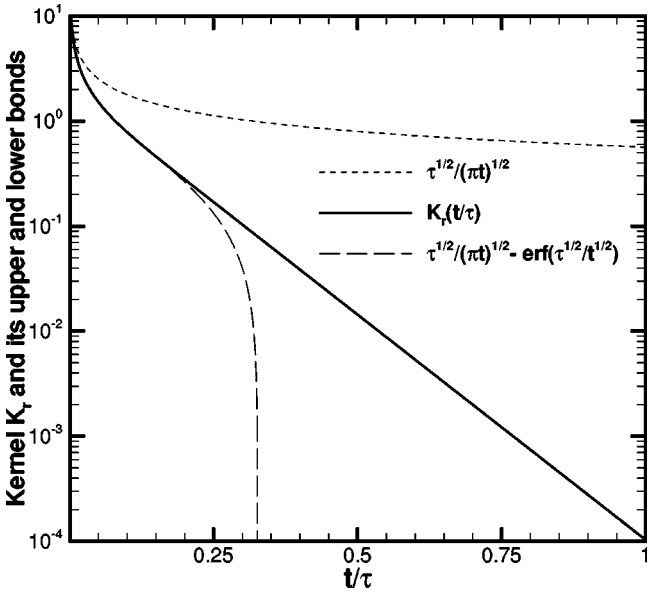

FIG. 1. Bounds and asymptotic behavior of kernel $K_r(t/\tau)$.

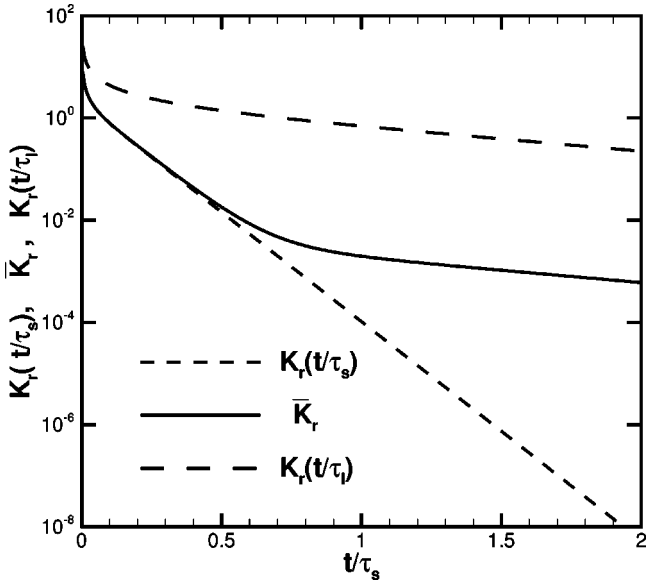

FIG. 2. Behavior of average kernel in a system with bimodal segment length distribution. The long to short segment length ratio is 3.0 and the long segment to short segment volume ratio is 2.4×10^{-2}.

$$\lim_{t\to 0} \bar{K}_r(\mathbf{x},t)\sqrt{t}=C, \tag{3.36}$$

where C is a positive number. In other words, the kernel $\bar{K}_r$ is proportional to $1/\sqrt{t}$ for a small time t.

The relaxation time τ in the history integrals is assumed to be constant during the deformation from time 0 to t. In many polymers, the friction coefficient C_f, thus the relaxation time τ, is sensitive to temperature. The heat produced during the deformation could result in a temperature increase in the polymer, especially in the cases of high-strain-rate motions. The effects of temperature change are not considered in the present paper and are a subject of further research.

IV. EFFECTS OF SEGMENT LENGTH DISTRIBUTION

In a polymer system the segment length is usually widely dispersed and so are the relaxation times for the segments according to Eq. (3.22). To understand basic effects of the segment length distribution, we first study a bimodal distribution with short segment length ℓ_s and long segment length ℓ_ℓ. For this case the probability distribution of segments P_s takes the following form:

$$P_s(r,\mathbf{x},t)=\left[\frac{N_s}{4\pi\ell_s^2}\delta(r-\ell_s)+\frac{N_\ell}{4\pi\ell_\ell^2}\delta(r-\ell_\ell)\right]n(\mathbf{x},t), \tag{4.1}$$

where $n(\mathbf{x},t)$ is the number density of segment end points while N_ℓ and N_s are, respectively, the average numbers of long and short segments connected to the point $\mathbf{x}$. Using Eq. (3.33), the average kernel can be calculated as

$$\bar{K}_r(t)=\frac{K_r(t/\tau_s)+\dfrac{N_\ell\ell_\ell}{N_s\ell_s}K_r(t/\tau_\ell)}{1+\dfrac{N_\ell\ell_\ell}{N_s\ell_s}}, \tag{4.2}$$

where τ_s and τ_ℓ are the relaxation times for the short and long segments calculated using Eq. (3.22). The ratio $N_\ell\ell_\ell^3/N_s\ell_s^3$ can be regarded as the volume ratio of the two different segments. In Fig. 2, we show the variation of $\bar{K}_r(t)$ using $\ell_\ell/\ell_s=3$ and $N_\ell/N_s=9\times10^{-4}$, with a corresponding long segment to short segment volume ratio of 2.4×10^{-2}. In this figure, it is shown that, for a very short time ($t/\tau_s<0.1$ in the figure) the average kernel behaves like $1/\sqrt{t}$. After that ($0.1<t/\tau_s<0.5$) the kernel behaves like an exponential with the relaxation time controlled by the short segments. After a transition period ($t/\tau_s>1$), the kernel behaves like exponential again with the relaxation time controlled by the long segments. Even though, in the example plotted in Fig. 2, the volume ratio of long segments is small (2.4×10^{-2}) compared to the short one, long segments still control the long relaxation time.

In the sense of a generalized distribution, we choose a set of segment lengths ℓ_i, and expand the probability distribution P_s as

$$P_s(r,\mathbf{x},t)=n(\mathbf{x},t)\sum_{i=1}^{\infty}\frac{N_i}{4\pi\ell_i^2}\delta(r-\ell_i), \tag{4.3}$$

where N_i is the average number of segments with length ℓ_i connected to the segment end point $\mathbf{x}$. With expansion (4.3), we calculated

$$\overline{K}_r(t)=\sum_{i=1}^{\infty}\beta_i K_r(t/\tau_i), \tag{4.4}$$

where

$$\beta_i=\frac{N_i\ell_i}{\sum_{i=1}^{\infty}N_i\ell_i}, \quad \sum_{i=1}^{\infty}\beta_i=1, \tag{4.5}$$

and τ_i is the relaxation time corresponding to segment length ℓ_i calculated using Eq. (3.22).

For practical problems, not all terms in Eq. (4.4) are important; only those terms with relaxation times of the same order of magnitude as the time scale of each problem are important. For a term with small relaxation time compared to the problem time scale, the kernel can be approximated as a δ function in time, and the strain rate can be treated as a constant during the kernel relaxation time and thus can be taken out from the history integrals. Therefore, such a term is nearly proportional to the strain rate at a given time, and can be modeled as a viscous term. The terms in Eq. (4.4) associated with large relaxation times compared to the problem time scale have a more complicated behavior since they contain the fast relaxation parts, the parts proportional to $1/\sqrt{t}$ for a short time, and slow relaxation parts for large t. The fast relaxation part in the history integral, as mentioned above, can be treated as a viscous part. For the slow relaxation part, in the time scale of the practical problem, the kernel can be treated as a constant, and pulled out from the history integral. In this way the only thing left in the history integral is the strain rate, which can be integrated to be a strain. Therefore the slow relaxation part behaves as an elastic term during the time scale of the problem. As a consequence of this, depending on the range of time scales of a problem, only a few terms in Eq. (4.4) are significant. For a practical problem, we then combine the terms treated as a viscous stress in $\boldsymbol{\sigma}^J$ with the viscous stress from $\boldsymbol{\sigma}^V$, and write the total stress $\boldsymbol{\sigma}=\boldsymbol{\sigma}^R+\boldsymbol{\sigma}^V+\boldsymbol{\sigma}^J$ in the polymer system as

$$\boldsymbol{\sigma}=(\lambda_R+\lambda_e)\mathrm{tr}(\boldsymbol{\epsilon})\mathbf{I}+2\lambda_e\boldsymbol{\epsilon}+\mu_e\dot{\boldsymbol{\epsilon}}+\lambda_e \times\int_0^t\{tr[\dot{\boldsymbol{\epsilon}}(t-t')]\mathbf{I}+2\dot{\boldsymbol{\epsilon}}(t-t')\}K_e(t')dt', \tag{4.6}$$

where $\lambda_e(>\lambda_0)$ is the apparent Lamé coefficient containing effects of the kernels in Eq. (4.4) associated with long relaxation times, μ_e is the apparent viscosity containing effects of the terms in Eq. (4.4) associated with short relaxation time and

$$K_e(t)=\sum_{i=1}^{\infty}\alpha_i K_r(t/\tau_i), \quad \alpha_i=\frac{\lambda_0\beta_i}{\lambda_e}>0, \text{ and } \sum_{i=1}^{\infty}\alpha_i<1. \tag{4.7}$$

The terms contained in summation (4.7) belong to a subset of the terms contained in (4.4) with the relaxation times comparable to the time scale of the problem.

The derivation of expressions for stresses $\boldsymbol{\sigma}^V$ and $\boldsymbol{\sigma}^J$ have been based on the assumption of small deformations so that the pair distribution function is spherically symmetric. We have also dropped the nonlinear effect of $\boldsymbol{\epsilon}$ from $\boldsymbol{\sigma}^R$. As mentioned in Sec. III, λ_R is small compared to λ_e, so that for many practical purpose, λ_R can be neglected. As a consequence of this, this model predicts that the Poisson's ratio is about 0.25 for small deformations.

V. COMPARISON WITH EXPERIMENTS

Experiments described in this paper were performed independently from the theoretical development of this paper. The specimen was a nitroplasticized estane cylinder, 7.8 mm in height and 7.6 mm in diameter. Both ends of the specimen were well lubricated to ensure zero lateral stress during a uniaxial compression in the axial direction of the cylinder. The experiment was conducted at room temperature on an MTS-810 hydraulic testing machine. The largest strain rate in the compression was 3.3×10^{-2} s^{-1}. At such strain rates, the viscous stress and temperature change due to heat generation can be neglected, and the stress (4.6) can be written as

$$\sigma(t)=E_e\epsilon(t)+E_e\int_0^t\dot{\epsilon}(t-t')K_e(t')dt', \tag{5.1}$$

where $E_e=5\lambda_e/2$ is the effective Young's modulus.

In a compress-and-hold experiment, if the duration of the compression motion is short compared to the relaxation time, the strain rate can be approximated as

$$\dot{\epsilon}=\epsilon\delta(t). \tag{5.2}$$

The stress in this case can then be written as

$$\sigma(t)=\sigma_e[1+K_e(t)], \quad \sigma_e=E_e\epsilon. \tag{5.3}$$

The time dependent stress $\sigma(t)$ is measured in the experiment. Since K_e vanishes as time becomes large in Eq. (3.34), the stress σ_e is taken to be the stress $\sigma(t)$ at a sufficient long time when the change of its value is not significant. The kernel K_e can then be calculated using the measured stress $\sigma(t)$. The results are shown in Fig. 3. The experimental data can be fitted well using one term of K_r in Eq. (4.7).

$$K_e(t)=\alpha K_r(t/\tau), \quad \alpha=0.1, \quad \tau=1100 \text{ s}. \tag{5.4}$$

It is interesting to note that, in this case the relaxation time for the long decay, the exponential part, can be calculated as $\tau_a\approx111.1$ s, using definition (3.35). This time scale coincides with the time scale of this experiment, which is not accidental. As mentioned in Sec. 4, the complete kernel can be written as the summation of a series of K_r with different relaxation times, and only those terms with the relaxation times close to the time scales of the problem are significant.

To further illustrate the $1/\sqrt{t}$ behavior of the kernel for short times and to compare with experiments, we plot the kernel K_r and its experimental values in Fig. 4 with logarith-

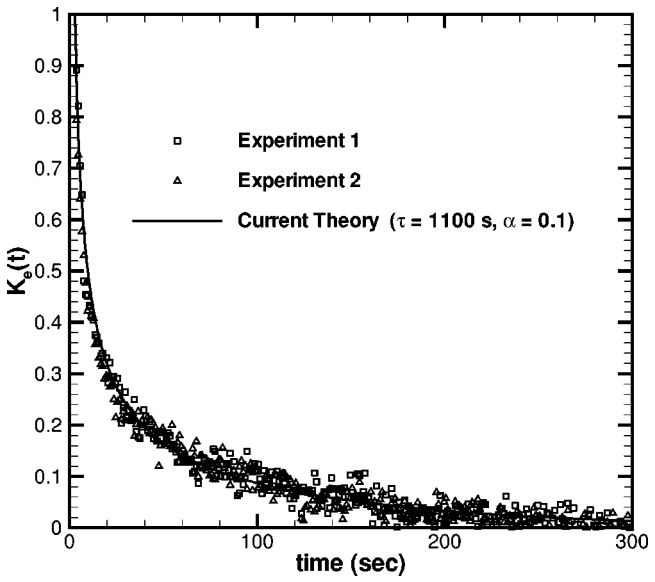

FIG. 3. Kernel K_e. The squares and triangles are the results calculated form two experiments. Both of the experiments were carried out by compressing the nitroplasticized estane specimen with a constant strain rate for 3.6 s and then recording the stress $\sigma(t)$ change with time for 302 s while holding the strain constant. The final strain in these experiments was 15.2%.

mic scales in both axes. The experimental values are shown to approach the straight line with slope $-1/2$, as predicted by our theory.

To illustrate the long time behavior of the kernel, we also plot K_e in Fig. 5 with logarithmic scale in the vertical axis. As mentioned before, for a large time, K_e approaches an exponential function, which is a straight line in the plot. The

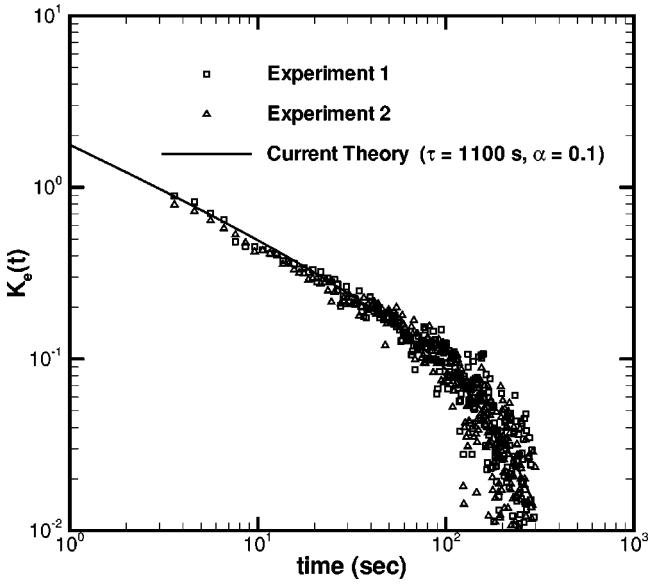

FIG. 4. The kernel K_e is plotted in a log-log scale. This figure illustrates the asymptotic behavior of K_e. It is shown that, as predicted by the current theory, as time t approaches zero, the experimentally obtained kernel indeed approaches a $1/\sqrt{t}$ asymptote, which is a straight line with slope $-1/2$.

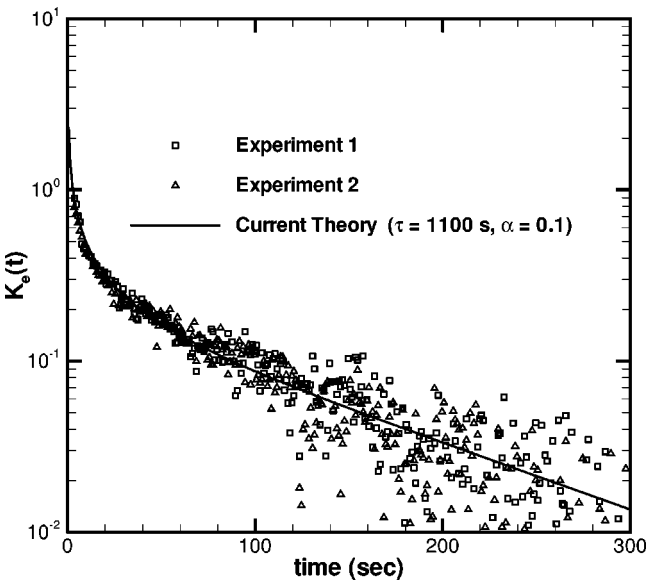

FIG. 5. To illustrate the long time behavior, in this figure both theoretical K_e and the experimental values are plotted in a logarithmic scale. The theoretical values are shown to form a straight line for large times, meaning K_e is asymptotic to an exponentially decaying function for large times. The experimental values scatter around the theoretical curve for large times. The scatter is due to the noise in the experiment, which becomes more visible in a logarithmic plot than in a normal plot for small values.

experimental values are seen to scatter around the theoretical curve in the figure. The scatter is due to the noise in the experiment, which becomes more visible in a logarithmic plot for small values.

With the relaxation time and coefficient of the kernel determined using experimental data, we use this kernel to calculated another compress-and-hold experiment with longer compression duration and lower strain rate than those of the experiments described above. The comparison of the calculated stress and the experimental results are shown in Fig. 6.

In many phenomenological models, the material is modeled as a series of Maxwell elements connected in parallel. In many numerical codes, it is numerically convenient to express the kernel in terms of decaying exponential functions, called a prony series. For this purpose, it is interesting to approximate the kernel derived in this paper in terms of a prony series as

$$K_r(t/\tau) \approx 0.74 \sum_{n=1}^{m} 10^{n/2} \exp(-10^n t/\tau), \qquad (5.5)$$

where m is determined by equating $10^{-m}\tau$ to the smallest time scale in the problem. Figure 7 shows the approximation to the kernel K_r using different values of m. Roughly speaking, Fig. 7 shows that a term per decade is needed to approximate the kernel derived in this paper.

VI. CONCLUSION

Beads in a polymer network are divided into bead groups represented by the end points of the segments to which the

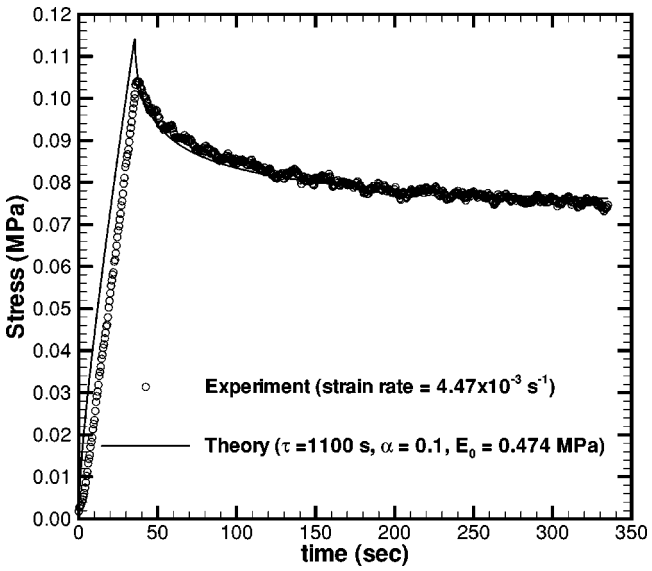

FIG. 6. Comparison of calculated stress and experimental values. The experiment was carried out by compressing nitroplasticized estane specimen with a constant strain rate for 35.5 s. The final strain is 15.3%.

beads belong. Macroscopic continuity and momentum equations are derived based on the interactions of the bead groups. Macroscopic stress can be divided into three parts. The first part represents the effects of velocity fluctuations of the beads in the system. The second part of the stress comes from interactions among bead groups, except for the interaction forces transmitted through the segments connecting them. The effect of the interaction forces transmitted through segments connecting different bead groups is represented by the third part. The interactions among the bead groups represented by the second part are transient while the segments connecting the bead groups are permanent. This difference in time scale enables us to model the interaction force between a bead and its surrounding beads belonging to other segments as a viscous force, and to model the second part of the stress as a viscous stress. To calculate the third part of the stres, one needs to model the average motion of segments. The potential and thermal motion of the beads in a segment results in a Helmholtz free energy. The tendency of the system to maintain a minimum free energy leads to thermal elasticity of the segment. Since the force acting on a bead from its surrounding medium can be modeled as a viscous force, the motion of the segment can be modeled as an elastic spring immersed in a viscous fluid. The inertia of the segment is neglected because it is small compared to the viscous force. For this reason, the equation of motion for an average segment can be written as a diffusion equation for the displacement. When the segment is pulled at the ends, the deformation takes time to diffuse toward the center of the segment; therefore the deformation is highly nonuniform in the average segment. This diffusion of deformation results in a history integral in the constitutive relation for the third part of the stress. After solving the diffusion equation, the kernel in the history integral is found to approach $\sqrt{\tau/t}$ for a short time t, and to approach a decaying exponential for a large time, where τ is the relaxation time related to the deformation diffusion. In this way, the constitutive relation for a solid polymer can be written in three terms, the viscous term, the elastic term, and the history dependent term. The relaxation time τ in the history dependent term is a function of the segment length. For a polymer, the segment length is widely dispersed and so is the spectrum of relaxation times. For a given practical problem, only a few relaxation times close to the time scale of the problem are significant. The stress associated with a short relaxation time can be modeled as a viscous stress and the stress associated with a long relaxation time can be modeled as an elastic stress.

The properties of our theoretically predicted kernel in the history integral are conformed by experiments.

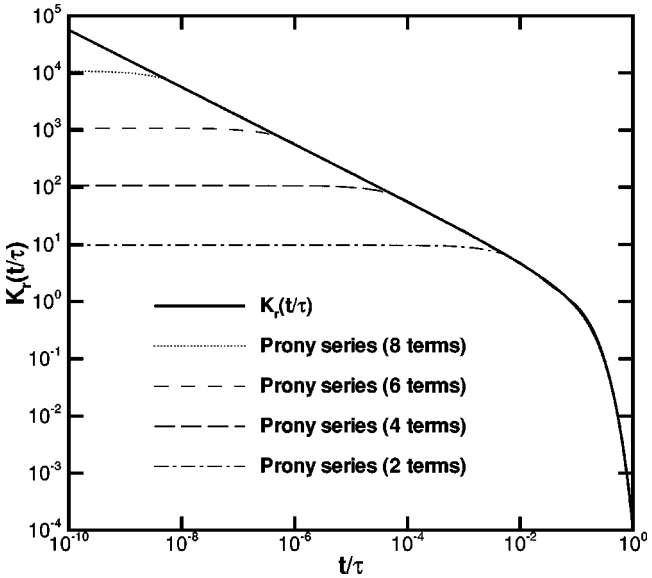

FIG. 7. Prony series approximation of the kernel.

ACKNOWLEDGMENTS

This work was supported financially by the United State Department of Energy and the Department of Defense/Office of Munitions under the Joint DoD/DoE Munitions Technology Development Program.

APPENDIX A

Theorem: Let F and $G_{\alpha\beta}$ be uniformly differentiable functions of $y_1, y_2, \ldots, y_n$, where α and β are two integers satisfying $1 \leqslant \alpha \leqslant n$ and $1 \leqslant \beta \leqslant n$. If the function $G_{\alpha\beta}$ satisfies

$$G_{\alpha\beta}(y_1, y_2, \ldots, y_\alpha, \ldots, y_\beta, \ldots, y_n) = -G_{\beta\alpha}(y_1, y_2, \ldots, y_\alpha, \ldots, y_\beta, \ldots, y_n), \tag{A1}$$

then there is a following identity:

$$\int \sum_{\alpha=1}^{N} \delta(x-y_\alpha) \sum_{\beta=1}^{N} F(y_1,y_2,\ldots,y_n) \times G_{\alpha\beta}(y_1,y_2,\ldots,y_n)dy_1dy_2\ldots dy_n = \frac{1}{2}\frac{d}{dx}\int \sum_{\alpha=1}^{N}\sum_{\beta=1}^{N} \delta(x-y_\alpha-h_{\alpha\beta})F(y_1,y_2,\ldots,y_n) \times G_{\alpha\beta}(y_1,y_2,\ldots,y_n)(y_\beta-y_\alpha)dy_1dy_2\ldots dy_n \tag{A2}$$

for a $h_{\alpha\beta}=\theta_{\alpha\beta}(y_\beta-y_\alpha)$, and $0<\theta_{\alpha\beta}<1$.

Proof: Let I be the integral on the left side of Eq. (A2). Since the integral is independent of α and β, by exchange roles of α and β, we have

$$I=\frac{1}{2}\int \sum_{\alpha=1}^{N}\sum_{\beta=1}^{N} [\delta(x-y_\alpha)F(y_1,y_2,\ldots,y_n) \times G_{\alpha\beta}(y_1,y_2,\ldots,y_n)+\delta(x-y_\beta)F(y_1,y_2,\ldots,y_n) \times G_{\beta\alpha}(y_1,y_2,\ldots,y_n)]dy_1dy_2\ldots dy_n. \tag{A3}$$

We note that the contribution from terms in which $\alpha=\beta$ is zero because of Eq. (A1). We now change integration variables as

$$r_\gamma=y_\gamma-y_1,\quad 1\leqslant\gamma\leqslant n \tag{A4}$$

and denote

$$F(y_1,y_2,\ldots,y_n)=f(y_1,r_2,\ldots,r_n), \tag{A5}$$

$$G_{\alpha\beta}(y_1,y_2,\ldots,y_n)=g_{\alpha\beta}(y_1,r_2,\ldots,r_n), \tag{A6}$$

then the integral becomes

$$I=\frac{1}{2}\int \sum_{\alpha=1}^{N}\sum_{\beta=1}^{N} [\delta(x-r_\alpha-y_1)f(y_1,r_2,\ldots,r_n) \times g_{\alpha\beta}(y_1,r_2,\ldots,r_n)-\delta(x-r_\beta-y_1)f(y_1,r_2,\ldots,r_n) \times g_{\alpha\beta}(y_1,r_2,\ldots,r_n)]dy_1dr_2\ldots dr_n, \tag{A7}$$

where we have used Eq. (A1). Upon integrating over y_1, we have

$$I=\frac{1}{2}\int \sum_{\alpha=1}^{N}\sum_{\beta=1}^{N} [f(x-r_\alpha,r_2,\ldots,r_n) \times g_{\alpha\beta}(x-r_\alpha,r_2,\ldots,r_n)-f(x-r_\alpha-r_{\alpha\beta},r_2,\ldots,r_n) \times g_{\alpha\beta}(x-r_\alpha-r_{\alpha\beta},r_2,\ldots,r_n)]dr_2\ldots dr_n, \tag{A8}$$

where

$$r_{\alpha\beta}=r_\beta-r_\alpha=y_\beta-y_\alpha. \tag{A9}$$

Upon using the Lagrangian theorem for the product of f and $g_{\alpha\beta}$, we have

$$I=\frac{1}{2}\int \sum_{\alpha=1}^{N}\sum_{\beta=1}^{N} \frac{\partial}{\partial x}[f(x-r_\alpha-h_{\alpha\beta},r_2,\ldots,r_n) \times g_{\alpha\beta}(x-r_\alpha-h_{\alpha\beta},r_2,\ldots,r_n)]r_{\alpha\beta}dr_2\ldots dr_n, \tag{A10}$$

where $h_{\alpha\beta}=\theta_{\alpha\beta}r_{\alpha\beta}$, and $0<\theta_{\alpha\beta}<1$. Since functions f and $g_{\alpha\beta}$ are uniformly differentiable, we can exchange the order of integration and differentiation and use the property of the δ function to write

$$I=\frac{1}{2}\frac{d}{dx}\int \sum_{\alpha=1}^{N}\sum_{\beta=1}^{N} \delta(x-r_\alpha-h_{\alpha\beta}-y_1)f(y_1,r_2,\ldots,r_n) \times g_{\alpha\beta}(y_1,r_2,\ldots,r_n)r_{\alpha\beta}dy_1dr_2\ldots dr_n. \tag{A11}$$

Using Eq. (A4) to change the integration variables back to $y_1,\ldots,y_n$, we obtain Eq. (A2) and prove the theorem.

Following a similar procedure, we can prove the following extension of the theorem.

Extension: For a uniformly differentiable vector function $\mathbf{G}^{\alpha\beta}$ of vector variables $\mathbf{y}^1,\ldots,\mathbf{y}^n$, if the following condition is satisfied:

$$\mathbf{G}^{\alpha\beta}=-\mathbf{G}^{\beta\alpha}, \tag{A12}$$

then

$$\int \sum_{\alpha=1}^{N} \delta(\mathbf{x}-\mathbf{y}^\alpha) \sum_{\beta=1}^{N} F(\mathbf{y}^1,\mathbf{y}^2,\ldots,\mathbf{y}^n)\mathbf{G}^{\alpha\beta}(\mathbf{y}^1,\mathbf{y}^2,\ldots,\mathbf{y}^n)d\mathbf{y}^1d\mathbf{y}^2\ldots d\mathbf{y}^n = \frac{1}{2}\boldsymbol{\nabla}\cdot\sum_{\alpha=1}^{N}\sum_{\beta=1}^{N}\int \delta(\mathbf{x}-\mathbf{y}^\alpha-\mathbf{h}^{\alpha\beta})F(\mathbf{y}^1,\mathbf{y}^2,\ldots,\mathbf{y}^n)\mathbf{G}_{\alpha\beta}(\mathbf{y}^1,\mathbf{y}^2,\ldots,\mathbf{y}^n)(\mathbf{y}^\beta-\mathbf{y}^\alpha)d\mathbf{y}^1d\mathbf{y}^2\ldots d\mathbf{y}^n, \tag{A13}$$

where $\mathbf{h}^{\alpha\beta}=\theta_{\alpha\beta}(\mathbf{y}^\beta-\mathbf{y}^\alpha)$, and $0<\theta_{\alpha\beta}<1$.

We now use this relation to prove Eq. (2.27) in Sec. II. According to definition (2.12) we have

$$\overline{n\sum_{\beta=1,\beta\neq\alpha}^{J}\mathbf{F}_a^{\alpha\beta}}=\int\sum_{\alpha=1}^{J}\sum_{\beta=1}^{J}\delta(\mathbf{x}-\mathbf{y}^{\alpha})\mathbf{F}_a^{\alpha\beta}(\mathcal{C},t)P(\mathcal{C},t)d\mathcal{C}. \tag{A14}$$

We now let $\mathbf{G}^{\alpha\beta}=\mathbf{F}_a^{\alpha\beta}$, $F=P$, and apply Eq. (A13) to find

$$\overline{n\sum_{\beta=1,\beta\neq\alpha}^{J}\mathbf{F}_a^{\alpha\beta}}=\frac{1}{2}\boldsymbol{\nabla}\cdot\int\sum_{\alpha=1}^{J}\sum_{\beta=1}^{J}[1+O(h^{\alpha\beta})]\times\delta(\mathbf{x}-\mathbf{y}^{\alpha})\mathbf{F}_a^{\alpha\beta}(\mathcal{C},t)(\mathbf{y}^{\beta}-\mathbf{x}^{\alpha})P(\mathcal{C},t)d\mathcal{C}. \tag{A15}$$

If the macroscopic length scale is large compared to the typical segment length, the effects of $\mathbf{h}^{\alpha\beta}$ can be neglected. With this assumption we find Eq. (2.27) in Sec. II by multiplying both sides of Eq. (A15) by $(1=)\int\delta(\mathbf{x}'-\mathbf{y}^{\beta})d^3x'$, exchanging orders of integration and, using definition (2.14). The conditionally average force $\langle\mathbf{F}_a\rangle_2$ is determined by

$$P_2(\mathbf{x}',\mathbf{x})\langle\mathbf{F}_a\rangle_2(\mathbf{x}',\mathbf{x})=\int\sum_{\alpha=1}^{J}\sum_{\beta=1}^{J}\delta(\mathbf{x}-\mathbf{y}^{\alpha})\delta(\mathbf{x}'-\mathbf{y}^{\beta})\times\mathbf{F}_a^{\alpha\beta}(\mathcal{C},t)P(\mathcal{C},t)d\mathcal{C}. \tag{A16}$$

The procedure used in the proof above is an extension of a similar result from Zhang and Rauenzahn [11] and Zhang and Prosperetti [13], where the result was limited to indistinguishable particle collections. That restriction is removed from the present proof.

APPENDIX B

In this appendix, we solve Eq. (3.21) with boundary and initial conditions (3.23), and study the properties of the solution. We assume that the displacement $\boldsymbol{\lambda}$ is along the direction connecting the two ends of a segment. To solve the equation, we first apply a Laplace transform with respect to time t to Eq. (3.21) and its boundary and initial conditions. Denoting s as the variable corresponding to t after the transformation, we have

$$s\hat{\lambda}=\frac{\ell^2}{4\tau}\frac{\partial^2\hat{\lambda}}{\partial x^2}, \tag{B1}$$

$$s\hat{\lambda}(\ell/2,s)=\hat{u}_e(s),\quad \hat{\lambda}(0,s)=0. \tag{B2}$$

The solution of Eq. (B1) with boundary conditions (B2) can be written as

$$\hat{\lambda}(x,s)=\frac{\hat{u}_e(s)\sinh(2x\sqrt{\tau s}/\ell)}{s\sinh(\sqrt{\tau s})}. \tag{B3}$$

The Laplace transformation of the force N can be calculated as

$$\hat{N}(\ell/2,s)=k_0\frac{\partial\hat{\lambda}}{\partial x}=\frac{2k_0}{\ell}\hat{u}_e(s)\sqrt{\frac{\tau}{s}}\coth(\sqrt{\tau s}). \tag{B4}$$

Using the convolution theorem, we have

$$N(\ell/2,t)=\frac{2k_0}{\ell}\int_0^t u_e(t')K\left(\frac{t-t'}{\tau}\right)dt', \tag{B5}$$

where

$$K\left(\frac{t}{\tau}\right)=L^{-1}\left[\sqrt{\frac{\tau}{s}}\coth(\sqrt{\tau s})\right]. \tag{B6}$$

We note that

$$\coth(\sqrt{\tau s})=\frac{1+\exp(-2\sqrt{\tau s})}{1-\exp(-2\sqrt{\tau s})}=[1+\exp(-2\sqrt{\tau s})]\times\left[1+\sum_{k=1}^{\infty}\exp(-2k\sqrt{\tau s})\right]=1+2\sum_{k=1}^{\infty}\exp(-2k\sqrt{\tau s}). \tag{B7}$$

Substituting Eq. (B7) into Eq. (B6) and then performing the inverse Laplace transformation, one finds

$$K\left(\frac{t}{\tau}\right)=\sqrt{\frac{\tau}{\pi t}}\left[1+2\sum_{k=1}^{\infty}\exp(-k^2\tau/t)\right]. \tag{B8}$$

We now study the properties of this kernel. Let $[x]$ be the integer part of x. We note that

$$\sum_{k=1}^{\infty}\exp(-k^2\tau/t)=\int_1^{\infty}\exp(-[x]^2\tau/t)dx. \tag{B9}$$

For $x\geqslant 1$, we have

$$\int_1^{\infty}\exp(-x^2\tau/t)dx<\int_1^{\infty}\exp(-[x]^2\tau/t)dx<\int_1^{\infty}\exp[-(x-1)^2\tau/t]dx. \tag{B10}$$

Using Eq. (B9), we can write Eq. (B10) as

$$\int_0^{\infty}\exp(-x^2\tau/t)dx-\int_0^{1}\exp(-x^2\tau/t)dx<\sum_{k=1}^{\infty}\exp(-k^2\tau/t)<\int_0^{\infty}\exp(-x^2\tau/t)dx. \tag{B11}$$

By changing variable to $\eta=x\sqrt{\tau/t}$, we see that

$$\int_0^{\infty}\exp(-x^2\tau/t)dx=\sqrt{\frac{t}{\tau}}\int_0^{\infty}\exp(-\eta^2)d\eta=\frac{1}{2}\sqrt{\frac{\pi t}{\tau}} \tag{B12}$$

and

$$\int_0^1 \exp(-x^2\tau/t)dx = \frac{1}{2}\sqrt{\frac{\pi t}{\tau}}\,\mathrm{erf}(\sqrt{\tau/t}), \qquad \text{(B13)}$$

where erf is the error function. With this, inequality (B11) can be written as

$$\frac{1}{2}\sqrt{\frac{\pi t}{\tau}}\,\mathrm{erfc}(\sqrt{\tau/t}) < \sum_{k=1}^{\infty} \exp(-k^2\tau/t) < \frac{1}{2}\sqrt{\frac{\pi t}{\tau}}, \qquad \text{(B14)}$$

where $\mathrm{efrc}(x) = 1 - \mathrm{efr}(x)$ is the complementary error function.

We now write

$$K\left(\frac{t}{\tau}\right) = 1 + K_r\left(\frac{t}{\tau}\right), \qquad \text{(B15)}$$

where

$$K_r\left(\frac{t}{\tau}\right) = \sqrt{\frac{\tau}{\pi t}}\left[1 + 2\sum_{k=1}^{\infty} \exp(-k^2\tau/t)\right] - 1. \qquad \text{(B16)}$$

Using Eq. (B14), we obtain

$$\sqrt{\frac{\tau}{\pi t}} - \mathrm{erf}\left(\sqrt{\frac{\tau}{t}}\right) < K_r\left(\frac{t}{\tau}\right) < \sqrt{\frac{\tau}{\pi t}}, \qquad \text{(B17)}$$

so that

$$\lim_{t\to\infty} K_r\left(\frac{t}{\tau}\right) = 0. \qquad \text{(B18)}$$

[1] R.H.W. Wientjes, R.J.J. Jongschaap, M.H.G. Duits, and J. Mellema, J. Rheol. **43**, 375 (1999).

[2] M. Doi and S.F. Edwards, *The Theory of Polymer Dynamics* (Clarendon Press, Oxford, UK, 1986).

[3] K.S. Schweizer, J. Chem. Phys. **91**, 5802 (1989).

[4] K.S. Schweizer, J. Chem. Phys. **91**, 5822 (1989).

[5] B.J. Berne, in *Statistical Mechanics, Part B: Time Dependent Processes*, edited by B.J. Berne (Plenum, New York, 1977), Chap. 5.

[6] S.A. Sukhishvili, Y. Chen, J.D. Müller, E. Gratton, K.S. Schweizer, and S. Granick, Nature (London) **406**, 146 (2000).

[7] A.A. Gurtovenko and Y.Y. Gotlib, Macromolecules **33**, 6578 (2000).

[8] E.N. Harstad, F.H. Harlow, and H.L. Schreyer, in *Thermal-hydraulic Problems, Sloshing Phenomena, and Extreme Loads on Structures*, edited by F. J. Moody, ASME Proceedings PVP 435 (American Society of Mechanical Engineers, New York, 2002), pp. 263–275.

[9] R.B. Bird, O. Hassager, R.C. Armstrong, and C.F. Curtiss, *Dynamics of Polymeric Liquids* (Wiley, New York, 1987).

[10] J.H. Irving and J.G. Kirkwood, J. Chem. Phys. **18**, 817 (1950).

[11] D.Z. Zhang and R.M. Rauenzahn, J. Rheol. **41**, 1275 (1997).

[12] D.Z. Zhang and R.M. Rauenzahn, J. Rheol. **44**, 1019 (2000).

[13] D.Z. Zhang and A. Prosperetti, Int. J. Multiphase Flow **23**, 425 (1997).

[14] D.Z. Zhang and A. Prosperetti, J. Fluid Mech. **267**, 185 (1994).

[15] D.A. McQuarrie, *Statistical Mechanics* (Harper & Row, New York, 1976).

[16] W.B. Russel, D.A. Saville, and W.R. Schowalter, *Colloidal Dispersions* (Cambridge University Press, Cambridge, England, 1989).

[17] F. Rodriguez, *Principles of Polymer Systems* (Taylor & Francis, London, 1996).